# Biogeochemical processes accounting for the natural mercury variations in the Southern Ocean diatom ooze sediments

Sara Zaferani[1], Harald Biester[1]

[1]Institut für Geoökologie AG Umweltgeochemie, Technische Universität Braunschweig, Braunschweig, 38106, Germany

*Correspondence to*: Sara Zaferani (s.zaferani@tu-braunschweig.de)

**Abstract.** Understanding the marine biogeochemical cycle of mercury is crucial as consumption of mercury enriched marine fish is the most important pathway of mercury uptake by humans. However, due to the lack of long term marine records, the role of the oceans in the global mercury cycle is poorly understood. ~~And w~~We do not have well documented data of natural mercury accumulations during changing environmental conditions, e.g. sea surface conditions in the ocean. To understand influence of different sea surface conditions (climate induced changes in ice coverage and biological production) on natural mercury accumulation, we used a continuous ~ 170 m Holocene biogenic sedimentary record from Adélie Basin, East Antarctica, which mainly consists of silica based skeletons of diatoms. We performed Principal Component Analysis and regression analysis on element concentrations and corresponding residuals ~~of element concentrations,~~ respectively to investigate the link between sediment mercury accumulation, terrestrial inputs, and productivity. Preindustrial mercury accumulation in the remote basin ~~pristine marine Antarctica~~ showed extremely high accumulation rates (median: 556 µg $m^{-2}$ $yr^{-1}$) that displayed periodic-like variations. Our analysis shows that the variations in total mercury concentrations and accumulation rates are associated with biological production and related scavenging of available water phase mercury by rapidly sinking algae or algae derived organic matter after intense algae blooms. High accumulation rates of other studied elements further revealed that in regions of high primary productivity, settling of biogenic materials removes many other elements from ocean surface (through scavenging or biological uptake). ~~In conclusion, t~~The link between mercury cycling and primary production will need to be considered in future studies of the marine mercury cycle under future primary production enhancement through climatic, temperature, and nutrient availability changes.

Commented [PM1]: Rewrite sentence

Commented [PM2]: Rewrite sentence

Commented [PM3]: Rewrite sentence

## 1 Introduction

Mercury (Hg) is a metal of environmental concern due to its ability to be transported from sources to background regions (predominantly ~~in~~ through the atmosphere) and ~~be transformed~~ its transformations into highly bioaccumulative and toxic methylated forms. In the biogeochemical cycle of Hg, the ocean, ~~as the dominant physical feature of our planet Earth,~~ is of specific concern. A substantial amount of Hg (~ 80 %) ~~which~~ is emitted to the atmosphere from natural and anthropogenic sources reaches the ocean (Horowitz et al., 2017; Schartup et al., 2019) and ocean sediments ~~have been~~ are considered ~~as~~ to be

Commented [PM4]: Reword

Commented [PM5]: Reword

an ultimate sink of Hg on a timescale of tens of thousands of years (Fitzgerald et al., 2007; Selin, 2009; Amos et al., 2013). Despite the critical role this sink process plays in the Hg biogeochemical cycle, little is known about the rates or amount of Hg accumulation in marine sediments, especially in the open ocean. In contrast to the well-studied Hg cycling in terrestrial environments, knowledge about the temporal and spatial distribution of Hg in the marine environment is limited to model estimations (Mason and Sheu, 2002; Sunderland and Mason, 2007) and water column measurements (Cossa et al., 2011; Lamborg et al., 2014). A main reason for our limited understanding of the fate of Hg in the oceans is the lack of high resolution marine sedimentary records, especially from the deep ocean (Zaferani et al., 2018).

The Hg input to the ocean is primarily through atmospheric deposition (Mason et al., 1994; Driscoll et al., 2013). After deposition, as either mercuric ion ($Hg^{2+}$) or elemental Hg ($Hg^0$), Hg can be (i) reduced to $Hg^0$ and evaded to the atmosphere, or (ii) scavenged from the water column by particulate matter and eventually buried in deep sea sediments, or (iii) methylated to either monomethylmercury ($CH_3Hg^+$) or dimethylmercury ($(CH_3)_2Hg$) (Mason et al., 2012; Lamborg et al., 2014). While models may differ in their predicted Hg values in the surface, subsurface and deep ocean, they all agree that the flux of Hg to the deep ocean is low (Lamborg et al., 2002; Mason and Sheu, 2002; Sunderland and Mason, 2007; Amos et al., 2013). Mason and Sheu (2002) estimated that almost 96 % of the atmospheric Hg flux to the ocean is lost through re-emission from the ocean surface, and only 30 % of the Hg flux that reaches the deep ocean is preserved in sediments. However, available data sets on Hg fluxes to the deep ocean and accumulation rates in deep ocean sediments are limited and applying the model estimates across the entire ocean introduces substantial uncertainty.

Commented [PM6]: Reword

One area in particular that highlights this uncertainty is the underestimation of the role of biological productivity in the global Hg cycle. The marine biogeochemical cycle of many elements (Morel and Price, 2003), including Hg (Lamborg et al., 2016; Zaferani et al., 2018), in seawater is controlled directly and indirectly by biological productivity. Regions of high biological productivity play an important role in the downward transport and burial of biologically essential and nonessential elements in the sediments of the deep sea (Schlesinger and Bernhardt, 2013). This assumption for Hg is supported by water column measurements. Lamborg et al. (2014) showed a nutrient nutrient-like distribution of Hg in the ocean water column of oceans. This study indicates that similar to carbon (C) and phosphorus (P), Hg shows higher concentrations in the deep water due to its release during organic matter decomposition. This can be due to the Hg—phytoplankton interactions and taking up uptake of Hg from the water phase by phytoplankton (Le Faucheur et al., 2014; Mason et al., 1996). This interaction controls the flux of Hg from the water column to sediments in several ways. First, scavenging of Hg from surface water by particulate organic matter reduces the availability of $Hg^{2+}$ for reduction to $Hg^0$. So, the re-emission flux of $Hg^0$ from productive regions will be lower (Soerensen et al., 2016; Zaferani et al., 2018). Second, Hg scavenging by algae removes Hg from the dissolved phase and may shift the flux of Hg between the atmosphere and the ocean towards the dissolved phase by changing the dissolution equilibrium (Biester et al., 2018; Zaferani et al., 2018). Third, removal of dissolved Hg from the water column by algae and

other particulate matter facilitates the downward flux of Hg to the seafloor (Lamborg et al., 2016), which, as mentioned, has traditionally been considered to be slow in its nature. Thus, underestimating the role of biological productivity in the marine biogeochemical cycle of Hg may lead to an overestimation of re-emission fluxes from surface water and ~~underestimates~~ an underestimation of the Hg flux to deep sea sediments.

In this context, the Southern Ocean is of particular interest due to its high concentrations of nutrients and related elevated primary productivity (Arrigo et al., 1998). In the Southern Ocean, diatoms are major primary producers (Crosta et al., 2005). Their siliceous cell walls preserve well in sediments and form diatom ooze (Fütterer, 2006). The sedimentation rate of diatom ooze is high, estimated to reach up to 2 cm $yr^{-1}$ (Escutia et al., 2011). ~~This high sedimentation rate makes diatom ooze~~ making deposits around Antarctica a unique geochemical archive to study the influence of primary productivity on the accumulation of Hg as well as to entangle changes in the natural and anthropogenic marine biogeochemical cycle.

Despite providing a unique geochemical archive, studies on Hg cycling in the Southern Ocean, ~~and~~ particularly in the Antarctic region, are generally limited to ~~the~~ water column (Cossa et al., 2011) and ice core~~s~~ measurements (Vandal et al., 1993). Cossa et al. (2011) showed that Hg concentrations range between 0.63 and 2.76 pmol $L^{-1}$ in open water, 1.15 ± 0.22 pmol $L^{-1}$ in Antarctic Intermediate Water, and 1.35 ± 0.39 pmol $L^{-1}$ in Antarctic Bottom Water between the Antarctic continent and Tasmania. The observed variations in the vertical distributions of Hg were attributed to air-sea exchange and the affinity of Hg to bind to planktonic and inorganic particulate matter in the biologically productive zone. Hg concentrations in an ice core, covering the past 34 Kyr, varied between 0.0005 and 0.0021 µg $kg^{-1}$, corresponding to depositional fluxes of 0.009 and 0.031 µg $m^{-2}$ $yr^{-1}$ during the Holocene and the Last Glacial Maximum, respectively (Vandal et al., 1993). Vandal et al. (1993) attributed the observed enhanced Hg flux during colder periods to marine biological productivity and emissions of volatile Hg compounds from the ocean.

In a previous paper, we discussed the accumulation of anthropogenic Hg in ~~Adélie Basin~~ sediments of the Adélie Basin, offshore East Antarctica. The ~ 2-fold increase in Hg concentrations and accumulation rates in the upper ~ 2.80 m depth of the core was attributed to the onset of the industrial revolution and the strong increase in coal burning at ~ 1850 CE (Zaferani et al., 2018). Here we discuss the natural processes (e.g. changes in biogenic and terrestrial material fluxes) that controlled Hg accumulation in the same sediment core prior to 1850 CE throughout the past 8600 years. We investigated the continuous ~ 170 m long Holocene laminated diatom ooze sediment record from the Adélie Basin ~~offshore East Antarctica~~. Covering almost the entire Holocene, the core allows the determination of natural variations of ~~in~~ Hg accumulation rates in these sediments prior to major anthropogenic influences. Our main objective was to investigate the influence of different Hg sources, climate induced changes in biological productivity and terrestrial fluxes (through melting of glacier ice), which have controlled the sequestration of Hg in these sediments. To evaluate the influence of different biogeochemical processes on the Hg

**Commented [PM7]:** This can be condensed

**Commented [PM8]:** Reword

**Commented [PM9]:** This should be rewritten to explain the Hg distribution more clearly

accumulation in sediments, with an emphasis on the role of changes in planktonic productivity, we combined the data on Hg accumulation with data derived from multi element analyses.

## 2. Materials and methods

### 2.1 Study site and core collection

Sediments of the Adélie Basin were collected during the Integrated Ocean Drilling Program (IODP) Expedition from the hole U1357B 318 in 2010. ~~The hole~~ U1357B is located on the continental shelf off of Wilkes Land at the Mertz Glacier polynya (region~~s~~ of open water surrounded by sea ice), Antarctica (66°24.7990′ S, 140°25.5705′ E) at about 1021.5 m water depth (Escutia et al., 2011) (Fig 1). The total length of the recovered core is 170.7 m, corresponding to nearly the entire Holocene (Escutia et al., 2011). The core was sliced by 5c$m^3$~~e~~ plastic scoops (1cm wide samples). Samples in the upper core (3.2–25.05 mbsf) were taken at a resolution of ~ 20 years and at resolutions of ~ 200 years in deeper sections (25.05–170.35 mbsf), resulting in a total of 78 samples.

The sediment core is characterized by light and dark laminations which are undisturbed by sea level changes or glacial erosion (Denis et al., 2006; Escutia et al., 2011). Light laminations correspond to spring seasons when light and high nutrient~~s~~ levels promote intense phytoplankton blooms and are mainly composed of biogenic materials~~, i.e.~~ (mostly diatom with minor abundance of silicoflagellates, sponge spicules, radiolarians, and foraminifers). ~~Whereas d~~Dark layers correspond to the summer/autumn season when sea ice has retreated, and nutrient levels are low. Dark laminations are composed of a mixture of biogenic and terrigenous materials resulting from summer production in open water, ~~and~~ with glacial and subglacial inputs, respectively. High levels of primary production in surface water of this region, coupled with rapid fluxes of biogenic debris~~,~~ directly to the seafloor, led to high sedimentation rates of up to 2.0 cm $yr^{-1}$ during the past 10,000 years (Escutia et al., 2011).

### 2.2 Analyses of mercury and major and trace metals

All samples were freeze dried and ground using a glass pestle prior to geochemical analysis. Total Hg was determined by thermal decomposition followed by pre-concentration of Hg on a gold trap and CVAAS Hg detection using a Milestone DMA80 analyzer (US EPA Method 1998). The quality of the analysis was ensured by including a certified reference material (CRM) (Canmet LKSD-4 = 190 ± 17 ng $g^{-1}$) alongside the analyzed samples. The average measured concentration for LKSD-4 was 197 ± 11 ng $g^{-1}$. Replicate analyses (n = 20) were always within an RSD of 10 % of the certified value.

The samples were analyzed for concentrations of silicon (Si), titanium (Ti), zirconium (Zr), sulfur (S), calcium (Ca), potassium (K), aluminum (Al), yttrium (Y), manganese (Mn), strontium (Sr), iron (Fe), lead (Pb), copper (Cu), zinc (Zn), arsenic (As), bromine (Br), nickel (Ni), chlorine (Cl), and rubidium (Rb) by ~~means of~~ energy dispersive X-ray fluorescence (ED-XRF). The

calibration method, accuracy, and precision are described in detail in Cheburkin and Shotyk (1996). The CRMs (Canmet LKSD-4, NRC/CNRC-PACS-2, NRC/CNR-Mess-3, and NCS-DC75304) and replicates were measured in each set of samples for accuracy and precision control. Repeated analysis of CRMs gave relative standard deviation (SRD) less than 10 % for Si, Al, Ca, Y, Sr, Zr, Br, and Rb, 6–15 % for Ti, K, Zn, S, Fe, Mn, and Pb, 6–19 % for Cl, 10–20 % for Ni, 9–14 % for Cu, and 14–22 % for As.

### 2.3 Statistical analyses

Principal component analysis (PCA) was applied to the major and trace element concentrations to identify processes controlling the variability of elements in the sediments. When there is a complex set of variables, PCA is used to reduce a large number of variables to a new set of artificial variables, called principal components. Each component includes variables with a similar down core pattern. The principal components are then interpreted in terms of relevant geochemical processes that can control the variability of the major and trace elements in the sediments. The derived interpretation from PCA was then combined with the Hg data to examine the processes that could affect Hg accumulations. The analysis was performed on the standardized concentration data using Z-scores.

Commented [PM10]: This should be defined

Regressions analysis of the corresponding residuals was used~~, too~~ to establish the important elemental relationships, by considering Si concentration as an independent variable and other element concentrations as dependent variables. Correlation analysis and PCA were performed using the statistical software SPSS 25.0.

## 3. Results and discussion

### 3.1 Elemental composition of the diatom ooze sediments and geochemical processes controlling their distribution

Concentration profiles and accumulation rates of Si, Al, K, Ti, S, Ca, Zn, Fe, Br, As, and Cl are shown in Fig. 2-5 and discussed in supplementary materials. The preindustrial geochemical record of Adélie Basin sediments is generally characterized by periodic-like variations in the relative abundance of major and trace elements. The records of element accumulation rates largely follow those of periodic-like variations of concentrations and show no significant trend with depth (except Cl).

Commented [PM11]: These figures should be discusse throughout this section

The PCA resulted in five components, explaining almost 82 % of the total variance (Table 1). The first component (Cp1), explains 33 % of the variance and shows large (> 0.7) positive loadings of Mn, Ti, Rb, Zr, K, and Y and moderate positive loading of Fe. The second component (Cp2), which explains 20 % of the variance, is characterized by large positive loadings of Al, Si, S, and Cl and moderate positive loading of K and Ca. The third component (Cp3) explains 17 % of the variance and shows large positive loadings of Zn, Cu, and Ni and moderate positive loading of Fe. The fourth and fifth components (Cp4 and Cp5) account for 7 and 5 % of the variance, respectively. Cp4 is characterized by high positive loadings for Hg and As and moderate negative loading of Pb. Cp5 shows positive loadings for Sr and Ca.

In general, results of PCA imply that opening and closing of the polynya and biological production are the most important factors influencing sedimentation in the Adélie Basin. This has been shown by loadings of elemental proxies for terrigenous and biological material inputs. Briefly, Cp1, which includes positive loadings of lithogenic elements, represents the variability of terrigenous inputs. Melting of ice releases trapped lithogenic material into the water and leads to the sinking of lithogenic particles and their sedimentation. Cp2 comprises loading of elements of both biogenic and terrigenous sources. This component appears to reflect phytoplankton blooms and export of biological materials. After ice melt, when the ice is opening, favorable conditions for biological productivity lead to phytoplankton blooms and export of biogenic materials to the seafloor (Denis et al., 2006). Biogenic material is mainly biogenic silica because diatoms are a major component of blooms in the Adélie Basin (Escutia et al., 2011). The sinking of diatoms from the surface and their sedimentation can cause scavenging of elements during bloom time. Al shows positive loadings in this component rather than in Cp1. This, other than association with the flux of aluminosilicates material can also be attributed to the scavenging of Al by diatom particles (Moran and Moore, 1992). Cl also shows loading in Cp2. The possible explanation for the observed covariation is that marine phytoplankton is rich in polyunsaturated lipids and can account as chlorination substrates (Leri et al., 2015). However, the organic C content of Adélie Basin sediments is generally low (between 1 and 2 wt %), and some of the Cl must be in an inorganic form trapped in sediments owing to high sedimentation rates. Cp3 is mainly characterized by elements that are associated with the organic fraction of diatom cells. This component appears to reflect the remineralization process. Trace elements associated with organic parts of cells can be released back into the water column during decomposition. Therefore, cellular locations of elements, i.e. opal frustules of diatoms or organic matter of diatom cells, created different components of Cp2 and Cp3. Cp4 consists of particle reactive metals, e.g. Hg and Pb. The possible explanation for not having these two particle reactive metals in Cp2 is that these two metals begin to enter the system after ice melting, while Cp2 shows scavenging of elements by diatoms that are already present in the water column. Since Pb and Hg are negatively correlated, this component cannot reflect a pollution signal. Covariation of Ca and Sr in Cp5 represents sedimentation of planktonic foraminifera, which appears to be of minor importance here.

Cp1 explains 33 % of the variance and accounts for much of the variability/process which controlled the geochemical composition of these sediments. However, the high concentration of Si and low concentrations of terrigenous elements imply that in an environment like Adélie Basin, with extremely high productivity, input of lithogenic materials is changing while different diatom~~s~~ taxa are always present in the system, e.g. as sea ice associated and open ocean diatom.

Although the core was not sampled at one year resolution, the fluctuations of elemental concentrations are likely related to the seasonal variation of sea surface conditions like ice melting and freezing and its subsequent biological or terrestrial material~~s~~ exports. Sampling in light (associated with spring ~~seasons~~) or dark (associated with summer/autumn ~~seasons~~) laminae, which contain different amounts of biogenic or terrestrial materials can cause the observed variations (see Sect. 2.1).

**Commented [PM12]:** Reword

The element concentrations are comparable to other published sediment data, while the accumulation rates are much higher than other reported values. The existence of rapidly settling particles in Adélie Basin can explain the high element accumulation rates. The ~~high accumulation~~ rates suggest that most elements in the water column of Adélie Basin are subjected to removal by intense phytoplankton blooms through consumption or scavenging. Aggregation of diatoms, which creates large particles, ~~and their~~ sink~~ing~~ to the seafloor and can create a space in which elements can be trapped (Shanks and Trent, 1979). This enhances removal of elements from the water column and their sedimentation as well.

### 3.2 Holocene record of mercury concentrations and accumulation rates

In the preindustrial period, i.e. from the bottom of the core at ~ 170 m to 2.80 m depth (8600 years ago to ~ 1850 CE), the Hg record shows no obvious trend with depth but rather periodic-like variations. Hg concentrations fluctuate ~~by a factor of about 2~~ between 12.6 and 21.1 µg $kg^{-1}$ within 170-137 m depth and between 21.7 and 44.6 µg $kg^{-1}$ within 137–2.80 m depth of the core, with two more pronounced peaks at around 9.99 and 8.20 m depth. The lower concentration of Hg within 170-137 m depth of the core is probably attributed to the cooler ~~condition~~ temperature and sea ice cover during this period. Hg accumulation rates in the preindustrial period largely follow the Hg concentration record, with a median of 556 µg $m^{-2}$ $yr^{-1}$.

**Commented [PM13]:** Reference relevant figures

**Commented [PM14]:** Reference?

The high preindustrial Hg accumulation rates in Adélie Basin sediments cannot be explained by preindustrial atmospheric Hg depositions alone, which did not exceed 20 µg $m^{-2}$ as recorded in an Antarctic ice core (Vandal et al., 1993). Therefore, non-atmospheric sources, such as dissolved water phase Hg or terrestrial inputs, are needed for Hg enrichment in these sediments.

To identify driving forces behind the variations in Hg accumulation we used our PCA results. PCA demonstrated that two main processes, i.e. biogenic productivity and lithogenic inputs, controlled the flux of elements to Adélie Basin sediments. The component scores, which illustrate the depth dependency of the extracted components, are characterized by see-saw patterns throughout the entire core. This indicates different contributions of biogenic and terrigenous inputs most likely associated with spring and summer/autumn seasons, respectively.

The variance of Hg was not captured by Cp1, Cp2 or Cp3. Hg instead forms a group on Cp4 together with positive loading of As and negative loading of Pb. The absence of significant loading of Hg on Cp1, Cp2, and Cp3 (Table 1) and the lack of similarity between component scores and Hg concentrations (Fig. 7 and 8), in the preindustrial period, indicates that Hg fluxes are not significantly influenced by changes in lithogenic inputs through ice melting. These results further indicate that changes in the contribution of biogenic material also do not directly explain the variation of Hg accumulation in the sediments. The main reason for not finding any statistical relation between Hg and biogenic materials is that the amount of algal material during ~~algae~~ blooms is always large and therefore not a limiting factor for the scavenging of Hg. There has always been excess algal material within or passing through the water column to scavenge all water column Hg. Thus, we assume that nearly all

Hg in the water column is removed through scavenging during diatom blooms, but that Hg scavenging events do not or less frequently occur during summer/autumn seasons when primary productivity is lower and open ice expansion is at its maximum. Similar to other elements, the periodic-like variations observed in the preindustrial Hg record are likely attributed to the sampling variability at seasonal scales and laminae, which have different contents of biogenic and terrestrial materials. This can affect Hg concentrations. However, investigation at seasonal resolution is needed to further confirm our observations.

To calculate the maximum amount of Hg which could be ~~at maximum~~ scavenged by a single bloom event we used the Hg concentration of 271 ± 78 pg $L^{-1}$ in Antarctic Bottom Water, as suggested by Cossa et al. (2011). A water column of one $m^2$ and 1000 m depth would then amount to 271 ± 78 µg $m^{-2}$. This means that only about 2-3 algae blooms and scavenging events per year are necessary to obtain the average Hg accumulation rate in Adèlie Basin diatom ooze sediments, i.e. 556 ± 137 µg $m^{-2}$ $yr^{-1}$. This appears to be likely taking into account that the sinking speed of diatom agglomerates at Adélie Basin has been reported to reach 100-400 m per day (Jansen et al., 2018). Formation of Antarctic bottom water which is linked to the polynyas (Ohshima et al., 2013) can rapidly "refill" the Hg inventory in the water column after a scavenging event. This calculation suggests the high Hg accumulation rates in the Adélie Basin sediments can be solely explained by scavenging of water column Hg and does not need an additional atmospheric or terrestrial source. Nevertheless, we assume that similar to $CO_2$, Hg fluxes from the atmosphere will increase during algae blooms as a result of continuous removal of dissolved phase Hg by diatom particles and the resulting shift of the dissolution equilibrium towards the dissolved phase which should additionally increase the Hg flux from the atmosphere into the water. Hg removal from the upper water ~~phase~~ column by diatom organic matter will also decrease Hg re-evasion to the atmosphere as previously assumed in a model study (Soerensen et al., 2016).

## 4. Conclusions

Investigation of biogenic sediments revealed that biological productivity and related scavenging of water phase Hg by rapidly sinking algae or algae derived organic matter controlled preindustrial Hg accumulation in Adélie Basin, Antarctica. Our study suggests that the periodic-like variations in total Hg concentrations and accumulation rates are likely associated with the cycle of polynya opening and closing and its related changes in biological productivity. Although the high Hg accumulation in diatom ooze does not represent the Hg sedimentation process across all the world's oceans, our data shows that Hg scavenging by algae or sinking algae derived organic matter is a key process controlling the sequestration of Hg in marine sediments; and therefore the marine biogeochemical cycle of Hg in general. This can be similar to the association between very high benthic organic C fluxes with diatom production at the surface water which can be accelerated by aggregation (Sachs et al., 2009).

Our observations also suggest that re-emission of Hg from ocean surface waters as a result of reduction of Hg (II) might be reduced due to Hg scavenging by algae, at least in areas of high primary productivity. Moreover, Hg fluxes to marine sediments

**Commented [PM15]:** Reword

**Commented [PM16]:** Reword

might be higher than previously assumed in global model estimations. More data from marine sediments is needed to support this assumption. A future increase in marine productivity including algae blooms especially in coastal areas and semi-closed shallow seas will likely increase the Hg flux to bottom sediments. The model study of Soerensen et al. (2016) for the Baltic Sea might serve as an example for changes in marine Hg cycling caused by eutrophication.

*Author contributions.* Sara Zaferani carried out the experiments. Harald Biester encouraged and supervised the findings of this work. All authors contributed to a significant part to the presented scientific work.

*Competing interests.* The authors declare that they have no conflict of interest

*Acknowledgements.* This research was supported by TU Braunschweig. We thank P. Schmidt and A. Calean for technical assistance, Dr. DS. McLagan for the constructive comments.

**References**

Amos, H. M., Jacob, D. J., Streets, D. G. and Sunderland, E. M.: Legacy impacts of all-time anthropogenic emissions on the global mercury cycle, Global Biogeochem. Cycles, 27, 410–421, https://doi.org/10.1002/gbc.20040, 2013.

Arrigo, K. R., Worthen, D., Schnell, A. and Lizotte, M. P.: Primary production in Southern Ocean waters, J. Geophys. Res. Ocean., 103, 15587–15600, https://doi.org/10.1029/98JC00930, 1998.

Biester, H., Pérez-Rodríguez, M., Gilfedder, B. S., Martínez Cortizas, A. and Hermanns, Y. M.: Solar irradiance and primary productivity controlled mercury accumulation in sediments of a remote lake in the Southern Hemisphere during the past 4000 years, Limnol. Oceanogr., 63, 540–549, https://doi.org/10.1002/lno.10647, 2018.

Cheburkin, A. K. and Shotyk, W.: An energy-dispersive miniprobe multielement analyzer (EMMA) for direct analysis of Pb and other trace elements in peats, Fresenius. J. Anal. Chem., 354, 688–691, https://doi.org/10.1007/s0021663540688, 1996.

Chen, S.-Y., Ambe, S., Takematsu, N. and Ambe, F.: The chemical states of iron in marine sediments by means of Mössbauer spectroscopy in combination with chemical leachings, J. Oceanogr., 52, 705–715, https://doi.org/10.1007/BF02239461, 1996.

Cossa, D., Heimbu, L., Lannuzel, D., Rintoul, S. R., Butler, E. C. V, Bowie, A. R., Averty, B., Watson, R. J. and Remenyi, T.: Mercury in the Southern Ocean, Geochim. Cosmochim. Acta, 75, 4037–4052, https://doi.org/10.1016/j.gca.2011.05.001, 2011.

Crosta, X., Romero, O., Armand, L. K. and Pichon, J.-J.: The biogeography of major diatom taxa in Southern Ocean sediments: 2. Open ocean related species, Palaeogeogr. Palaeoclimatol. Palaeoecol., 223, 66–92, https://doi.org/10.1016/j.palaeo.2005.02.015, 2005.

Croudace, I. W. and Rothwell, R. G.: Micro-XRF Studies of Sediment Cores: Applications of a non-destructive tool for the environmental sciences, Springer., 2015.

Denis, D., Crosta, X., Zaragosi, S., Romero, O., Martin, B. and Mas, V.: Seasonal and subseasonal climate changes recorded in laminated diatom ooze sediments, Adelie Land, East Antarctica, The Holocene, 16, 1137–1147, https://doi.org/10.1177%2F0959683606069414, 2006.

Driscoll, C. T., Mason, R. P., Chan, H. M., Jacob, D. J. and Pirrone, N.: Mercury as a global pollutant: Sources, pathways, and effects, Environ. Sci. Technol., 47, 4967–4983, https://doi.org/10.1021/es305071v, 2013.

Escutia, C., Brinkhuis, H., Klaus, A. and Scientists, E. 318: Site U1357, Proc. Integr. Ocean Drill. Programprogr., 318, doi:10.2204/iodp.proc.318.105.2011, 2011.

Le Faucheur, S., Campbell, P. G., Fortin, C. and Slaveykova, V. I.: Interactions between mercury and phytoplankton: speciation, bioavailability, and internal handling, Environ. Toxicol. Chem., 33, 1211–1224, https://doi.org/10.1002/etc.2424, 2014.

Fitzgerald, W. F., Lamborg, C. H. and Hammerschmidt, C. R.: Marine biogeochemical cycling of mercury, Chem. Rev., 107, 641–662, https://doi.org/10.1021/cr050353m, 2007.

Fütterer, D. K.: The solid phase of marine sediments, in: Marine geochemistry, edited by H. D. Schulz and M. Zabel, pp. 1–25, Springer, Berlin, Heidelberg, https://doi.org/10.1007/978-3-662-04242-7_1%0A, 2006.

Horowitz, H. M., Jacob, D. J., Zhang, Y., DIbble, T. S., Slemr, F., Amos, H. M., Schmidt, J. A., Corbitt, E. S., Marais, E. A. and Sunderland, E. M.: A new mechanism for atmospheric mercury redox chemistry: implications for the global mercury budget, Atmos. Chem. Phys., 17, 6353–6371, https://doi.org/10.5194/acp-17-6353-2017, 2017.

Jansen, J., Hill, N. A., Dunstan, P. K., McKinlay, J., Sumner, M. D., Post, A. L., Eléaume, M. P., Armand, L. K., Warnock, J. P., Galton-Fenzi, B. K. and Johnson, C. R.: Abundance and richness of key Antarctic seafloor fauna correlates with modelled food availability, Nat. Ecol. Evol., 2, 71–80, https://doi.org/10.1038/s41559-017-0392-3, 2018.

Lamborg, C., Bowman, K., Hammerschmidt, C., Gilmour, C., Munson, K., Selin, N. and Tseng, C.-M.: Mercury in the Anthropocene Ocean, Oceanography, 27, 76–87, https://doi.org/10.5670/oceanog.2014.11, 2014a.

Lamborg, C. H., Fitzgerald, W. F., O'Donnell, J. and Torgersen, T.: A non-steady-state compartmental model of global-scale mercury biogeochemistry with interhemispheric atmospheric gradients, Geochim. Cosmochim. Acta, 66, 1105–1118, https://doi.org/10.1016/S0016-7037(01)00841-9, 2002.

Lamborg, C. H., Hammerschmidt, C. R., Bowman, K. L., Swarr, G. J., Munson, K. M., Ohnemus, D. C., Lam, P. J., Heimbürger, L., Rijkenberg, M. J. A. and Saito, M. A.: A global ocean inventory of anthropogenic mercury based on water column measurements, Nature, 512, 65–68, https://doi.org/10.1038/nature13563, 2014b.

Lamborg, C. H., Hammerschmidt, C. R. and Bowman, K. L.: An examination of the role of particles in oceanic mercury cycling, Philos. Trans. R. Soc. A Math. Phys. Eng. Sci., 374, 20150297, https://doi.org/10.1098/rsta.2015.0297, 2016.

Leri, A. C., Mayer, L. M., Thornton, K. R., Northrup, P. A., Dunigan, M. R., Ness, K. J. and Gellis, A. B.: A marine sink for chlorine in natural organic matter, Nat. Geosci., 8, 620–624, https://doi.org/10.1038/ngeo2481, 2015.

Lohan, M. C. and Tagliabue, A.: Oceanic micronutrients: trace metals that are essential for marine life, Elements, 14, 385–390, https://doi.org/10.2138/gselements.14.6.385, 2018.

Mason, R. and Sheu, G.-R.: Role of the ocean in the global mercury cycle, Global Biogeochem. Cycles, 16, 1–14, https://doi.org/10.1029/2001GB001440, 2002.

Mason, R. P., Fitzgerald, W. F. and Morel, F. M.: The biogeochemical cycling of elemental mercury: anthropogenic influences, Geochim. Cosmochim. Acta, 58, 3191–3198, https://doi.org/10.1016/0016-7037(94)90046-9, 1994.

Mason, R. P., Reinfelder, J. R. and Morel, F. M.: Uptake , Toxicity , and Trophic Transfer of Mercury in a Coastal Diatom, Environ. Sci. Technol., 30, 1835–1845, https://doi.org/10.1021/es950373d, 1996.

Mason, R. P., Choi, A. L., Fitzgerald, W. F., Hammerschmidt, Chad R Lamborg, C. H., Soerensen, A. L. and Sunderland, E. M.: Mercury biogeochemical cycling in the ocean and policy implications, Environ. Res., 119, 101–117, https://doi.org/10.1016/j.envres.2012.03.013, 2012.

Moran, S. and Moore, R.: Kinetics of the removal of dissolved aluminum by diatoms in seawater: A comparison with thorium, Geochim. Cosmochim. Acta, 56, 3365–3374, https://doi.org/10.1016/0016-7037(92)90384-U, 1992.

Morel, F. M. and Price, N.: The biogeochemical cycles of trace metals in the oceans, Science, 300, 944–947, https://doi.org/10.1126/science.1083545, 2003.

Morel, F. M. M., Reinfelder, J. R., Roberts, S. B., Chamberlain, C. P., Lee, J. G. and Yee, D.: Zinc and carbon co-limitation of marine phytoplankton, Nature, 369, 740–742, https://doi.org/10.1038/369740a0, 1994.

Ohshima, K. I., Fukamachi, Y., Williams, G. D., Nihashi, S., Roquet, F., Kitade, Y., Tamura, T., Hirano, D., HerraizBorreguero, L., Field, I., Hindell, M., Aoki, S. and Wakatsuchi, M.: Antarctic Bottom Water production by intense sea-ice formation in the Cape Darnley polynya, Nat. Geosci., 6, 235–240, https://doi.org/10.1038/ngeo1738, 2013.

Sachs, O., Sauter, E. J., Schlüter, M., Rutgers van der Loeff, M. M., Jerosch, K. and Holby, O.: Benthic organic carbon flux and oxygen penetration reflect different plankton provinces in the Southern Ocean, Deep. Res. Part I Oceanogr. Res. Pap., 56, 1319–1335, https://doi.org/10.1016/j.dsr.2009.02.003, 2009.

Schartup, A. T., Thackray, C. P., Qureshi, A., Dassuncao, C., Gillespie, K., Hanke, A. and Sunderland, E. M.: Climate change and overfishing increase neurotoxicant in marine predators, Nature, 572, 648–650, https://doi.org/10.1038/s41586-019-14689, 2019.

Schlesinger, W. H. and Bernhardt, E. S.: The Oceans, in: Biogeochemistry: an analysis of global change, pp. 341–395, Academic press., 2013.

Selin, N. E.: Global biogeochemical cycling of mercury: a review, Annu. Rev. Environ. Resour., 34, 43–63, https://doi.org/10.1146/annurev.environ.051308.084314, 2009.

Shanks, A. L. and Trent, J. D.: Marine snow: microscale nutrient patches 1, Limnol. Oceanogr., 24, 850–854, https://doi.org/10.4319/lo.1979.24.5.0850, 1979.

328 Soerensen, A. L., Schartup, A. T., Gustafsson, E., Gustafsson, B. G., Undeman, E. and Björn, E.: Eutrophication increases
329 phytoplankton methylmercury concentrations in a coastal sea - A Baltic sea case study, Environ. Sci. Technol., 50, 11787–
330 11796, https://doi.org/10.1021/acs.est.6b02717, 2016.

331 Sunderland, E. M. and Mason, R. P.: Human impacts on open ocean mercury concentrations, Global Biogeochem. Cycles, 21,
332 1–15, https://doi.org/10.1029/2006GB002876, 2007.

333 Vandal, G. M., Fitzgerald, W. F., Boutron, C. F. and Candelone, J.-P.: Variations in mercury deposition to Antarctica over the
334 past 34,000 years, Nature, 362, 621, https://doi.org/10.1038/362621a0, 1993.

335 Zaferani, S., Pérez-rodríguez, M. and Biester, H.: Diatom ooze—A large marine mercury sink, Science, 361, 797–800,
336 https://doi.org/10.1126/science.aat2735, 2018.

337

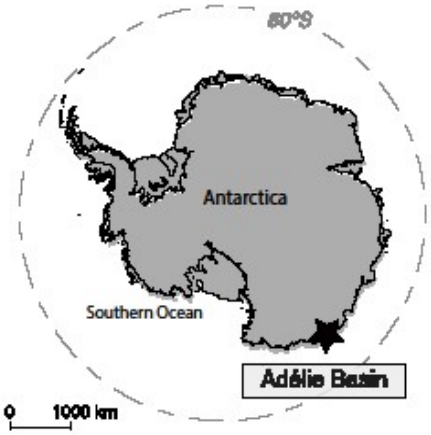


Figure 1: Map of Antarctica with the coring location of the IODP318-U1357B in Adélie Basin (Source: figure modified from Zaferani et al. (2018)).

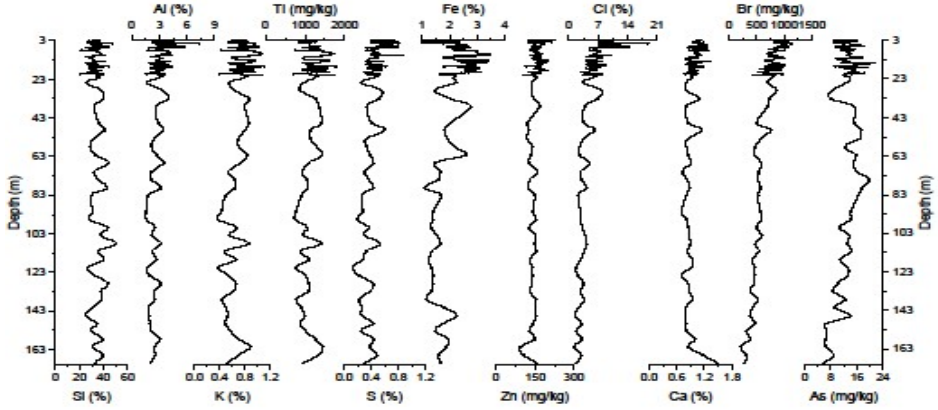


340

341 Figure 2: Down core records of Si, Al, K, Ti, S, Fe, Zn, Cl, Ca, Br, and As concentrations of Adélie Basin sediments.

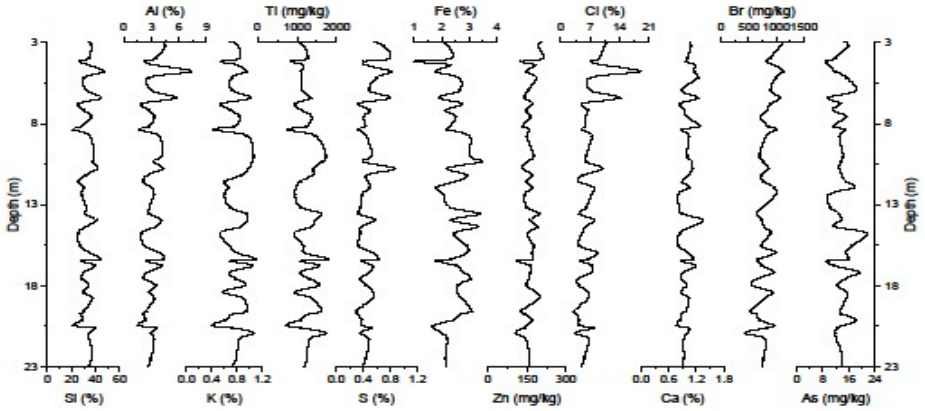


342

343 **Figure 3: Down core records of Si, Al, K, Ti, S, Fe, Zn, Cl, Ca, Br, and As concentrations of Adélie Basin sediments for the top 23 m**
344 **of the core.**

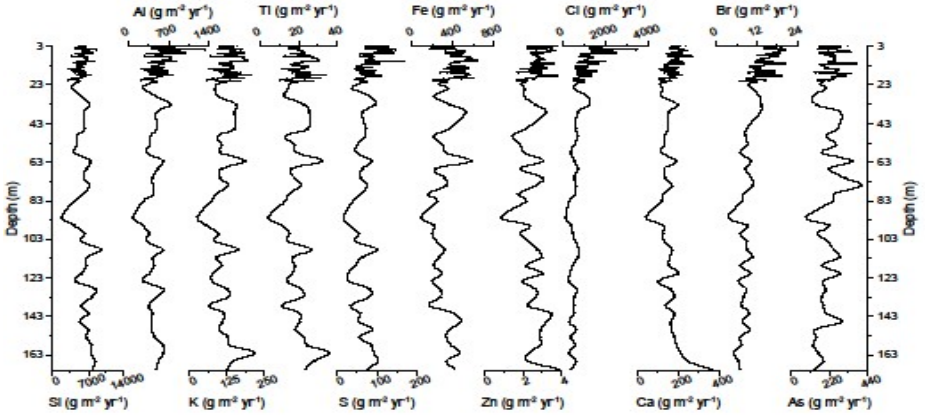


345

346 **Figure 4: Down core records of Si, Al, K, Ti, S, Fe, Zn, Cl, Ca, Br, and As accumulation rates of Adélie Basin sediments.**

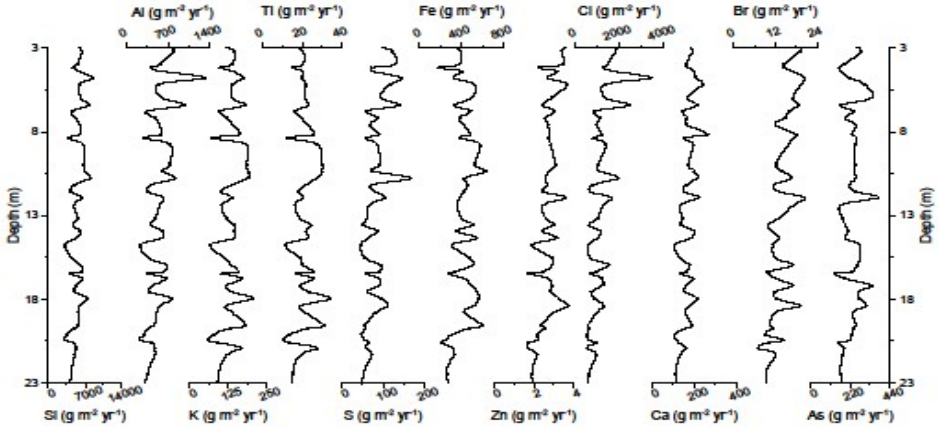


**Figure 5: Down core records of Si, Al, K, Ti, S, Fe, Zn, Cl, Ca, Br, and As accumulation rates of Adélie Basin sediments for the top 23 m of the core.**

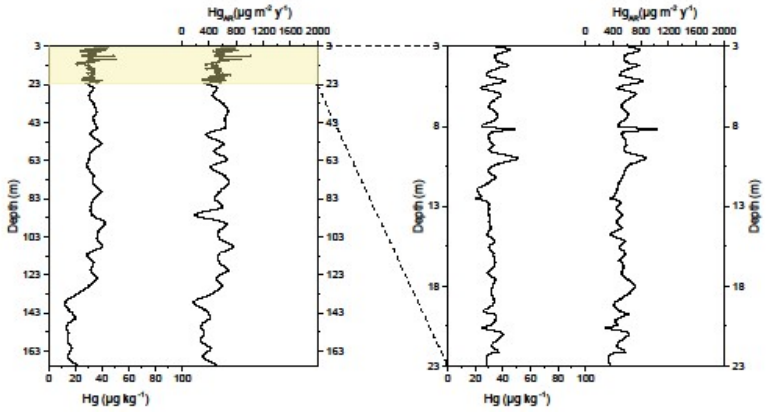


350

351 **Figure 6: Down core records of Hg concentrations and accumulation rates of Adélie Basin sediments.**

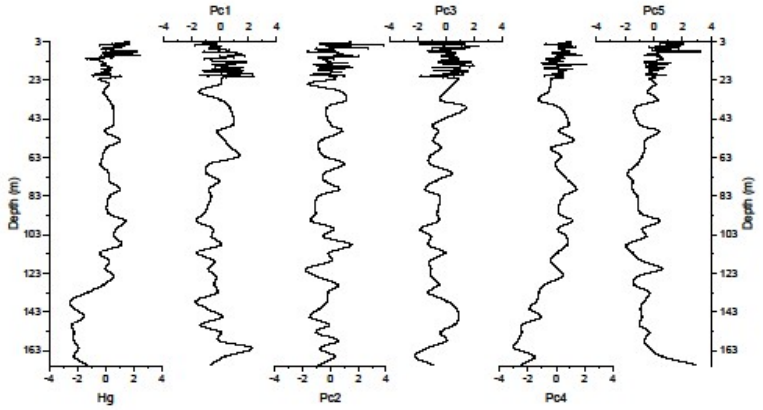


352

353 **Figure 7: Depth records of scores of the principal components extracted by PCA on the elemental composition of the sediments along**
354 **with Z-score of Hg of the Adélie Basin sediments.**

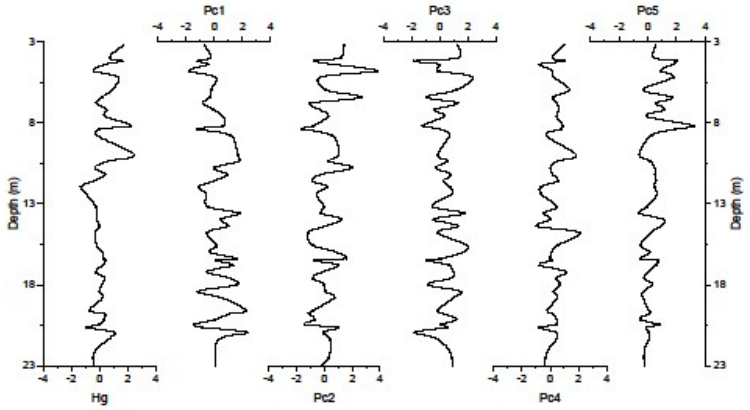


355

356 **Figure 8: Depth records of scores of the principal components extracted by PCA on the elemental composition of the sediments along**
357 **with Z-score of Hg of the Adélie Basin sediments for the top 23 m of the core.**

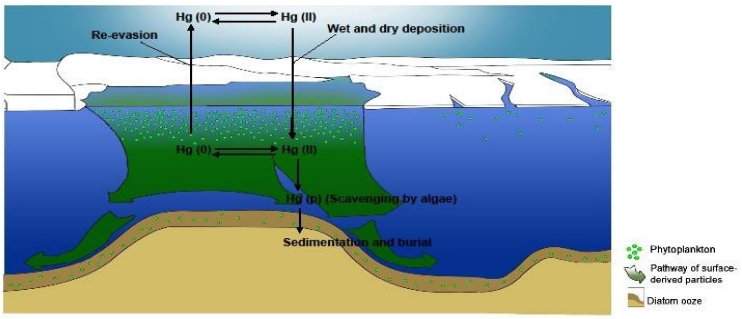


358

359 **Figure 9: Adélie Basin schematic Hg cycle model indicating the processes controlling Hg deposition and accumulation under high**
360 **primary production. Fast-sinking diatom particles remove dissolved water phase Hg from the water column through scavenging.**
361 **Hg removal from the dissolved phase by diatom particles will also decrease the Hg re-evasion to the atmosphere (Figure is adapted**
362 **from (Jansen et al., 2018).**

363 **Table 1: Factor loadings for the five significant components extracted by PCA from Adélie Basin sediment samples.**

| Elements | Components | | | | |
|---|---|---|---|---|---|
| | **1** | **2** | **3** | **4** | **5** |
| **Mn** | **0.89** | 0.40 | -0.05 | -0.05 | 0.01 |
| **Ti** | **0.89** | 0.43 | 0.01 | 0.04 | -0.02 |
| **Rb** | **0.84** | 0.03 | 0.39 | 0.10 | 0.20 |
| **Zr** | **0.83** | -0.22 | 0.05 | -0.15 | 0.08 |
| **K** | **0.73** | **0.66** | 0.05 | 0.08 | 0.10 |
| **Y** | **0.73** | -0.34 | 0.10 | -0.09 | 0.05 |
| **Al** | 0.12 | **0.93** | 0.06 | 0.05 | 0.18 |
| **Si** | 0.03 | **0.84** | -0.28 | -0.11 | -0.28 |
| **S** | 0.01 | **0.84** | 0.16 | 0.12 | 0.26 |
| **Cl** | -0.16 | **0.76** | 0.25 | 0.22 | 0.42 |
| **Zn** | -0.05 | 0.15 | **0.78** | 0.15 | 0.11 |
| **Cu** | 0.31 | 0.03 | **0.76** | 0.31 | 0.21 |
| **Ni** | 0.11 | -0.08 | **0.75** | -0.10 | 0.00 |
| **Fe** | **0.62** | 0.03 | **0.64** | 0.20 | 0.19 |
| **Br** | -0.23 | 0.35 | **0.50** | 0.46 | 0.48 |
| **Hg** | 0.17 | 0.09 | -0.04 | **0.79** | 0.14 |
| **As** | -0.01 | -0.09 | 0.30 | **0.73** | -0.26 |
| **Pb** | 0.35 | -0.11 | -0.10 | **-0.62** | -0.18 |
| **Sr** | 0.25 | 0.09 | 0.37 | 0.16 | **0.83** |
| **Ca** | 0.22 | **0.52** | -0.03 | -0.13 | **0.67** |
| **Eigenvalue** | 6.62 | 3.95 | 3.34 | 1.35 | 0.98 |
| **% variance** | 33.1 | 19.7 | 16.7 | 6.7 | 4.9 |

364